Skeletal Radiology (2019) 48:1043–1050
https://doi.org/10.1007/s00256-019-3145-3

SCIENTIFIC ARTICLE

B-cell peripheral neurolymphomatosis: MRI and ^{18}F-FDG PET/CT imaging characteristics

Anthony H. DeVries[1] · Benjamin M. Howe[1] · Robert J. Spinner[2,3] · Stephen M. Broski[1]

Received: 10 October 2018 / Revised: 27 December 2018 / Accepted: 1 January 2019 / Published online: 22 January 2019

Abstract

Objective To examine the MRI and ^{18}F-FDG PET/CT imaging characteristics of peripheral neurolymphomatosis.

Materials and methods All institutional cases of neurolymphomatosis with an MRI or ^{18}F-FDG PET/CT from 2000 to 2017 were retrospectively reviewed. Included cases were biopsy-proven neurolymphomatosis or lymphoma patients with clinical and imaging evidence of neurolymphomatosis that resolved after chemotherapy. Multiple imaging parameters and clinical characteristics were recorded.

Results There were 27 cases of B-cell neurolymphomatosis in 25 patients (18 M, 7 F; mean age 64.6 ± 10.0 years). Of the total cases, 85% (23/27) were biopsy-proven. Most were diagnosed after disease progression or recurrence (20/27, 74%), and presented with isolated nerve involvement (18/27, 67%). Bone marrow biopsy (17/19, 89%) and CSF cytology (16/23, 70%) were usually negative. On ^{18}F-FDG PET/CT, neurolymphomatosis presented as a linear or fusiform (23/26, 88%), FDG-avid (average SUVmax: 7.1 ± 4.5, range, 1.5–17.0) mass, and on MRI as a T2-weighted hyperintense (21/22, 95%), enhancing (21/22, 95%), linear or fusiform mass (19/22, 86%), with associated muscle denervation (14/22, 64%). FDG avidity was significantly higher in patients with muscular denervation on MRI (mean SUVmax 8.2 ± 4.6 vs. 4.3 ± 2.3, $p = 0.04$).

Conclusions B-cell neurolymphomatosis most commonly manifests as T2-weighted hyperintense, enhancing linear or fusiform neural enlargement associated with muscular denervation on MRI, with intense FDG activity on PET/CT. It is most often an isolated site of disease, presenting after progression or recurrence. A familiarity with the imaging appearance of neurolymphomatosis can help refine the differential diagnosis, direct biopsy, and aid in accurate diagnosis.

Keywords MRI · PET/CT · FDG · Neurolymphomatosis · Peripheral nerve · Lymphoma

Introduction

Neurolymphomatosis (NL) is an uncommon disease characterized by infiltration of the nervous system by lymphoma. Given the disease's rarity and complex diagnosis, its prevalence can only be estimated and ranges from 0.2% of all cases of NHL to 3% of new intermediate or high-grade cases [1, 2]. NL is most frequently associated with B-cell non-Hodgkin's lymphoma (NHL), though cases of non-B-cell NL have been reported [3–7]. In most patients, NL presents after several courses of treatment, and it is uncommonly a primary manifestation of lymphoma [3, 8].

Patients generally present with a painful neuropathy of the affected peripheral nerve [8, 9]. Diagnosis can be challenging given variable presenting symptoms [2, 4, 5, 9–13], the large differential diagnosis [14], and because cerebrospinal fluid (CSF) cytology and bone marrow biopsy are often negative [10, 11]. Additionally, the gold standard of nerve biopsy is invasive and carries a risk of permanent nerve damage [9, 12]. Therefore, imaging can play an important role in prompt diagnosis, help avoid unnecessary nerve biopsies, and also guide fascicular biopsy by identifying the highest yield target. Given the rarity of the disease, there has been minimal publication describing the imaging characteristics of NL, most of these being case reports [3, 15]. With the increasing use of MRI and ^{18}F-FDG PET/CT

✉ Stephen M. Broski
broski.stephen@mayo.edu

[1] Department of Radiology, Mayo Clinic, Charlton Building North, 1st Floor, 200 First Street SW, Rochester, MN 55905, USA

[2] Department of Neurosurgery, Mayo Clinic, Rochester, MN 55905, USA

[3] Department of Orthopedic Surgery, Mayo Clinic, Rochester, MN 55905, USA

in the evaluation of peripheral nervous system disorders, NL is increasingly being recognized [16]. Our aim was to evaluate the MRI and ^{18}F-FDG PET/CT imaging characteristics of peripheral neurolymphomatosis.

Materials and methods

With IRB approval, our institutional MRI and ^{18}F-FDG PET/CT databases were searched for cases of NL from 01/01/2000 to 12/31/2017. All cases where NL was mentioned in an MRI or ^{18}F-FDG PET/CT radiology report, pathology report, or clinic note were initially included in the cohort. Cases where NL was mentioned as a pertinent negative were then excluded. This cohort was reviewed and only patients with biopsy-proven NL or patients with biopsy-proven lymphoma at other sites with clinical and imaging evidence of NL that resolved on follow-up imaging after chemotherapy were included. MRI and ^{18}F-FDG PET/CT imaging characteristics were then evaluated by a board-certified radiologist with experience in both musculoskeletal MRI and PET/CT interpretation.

PET/CTs (Discovery RX, 690, or 710; GE Healthcare, Waukesha, WI, USA) were performed according to the standard clinical protocol. Weight, height, and blood glucose levels were recorded for all patients. All patients had a blood glucose level of less than 200 mg/dl and were injected with 10–15 mCi of ^{18}F-FDG, with an incubation period of 60-70 min. The amount of injected radioactivity was routinely measured by means of quantifying the radioactivity within the syringe before and after injection or with an automated injection system (Medrad® Intego PET infusion system, Bayer Healthcare, Whippany, NJ, USA). Patients were imaged covering at least from orbits to midthighs, (3D or 2D OSEM without TOF, two iterations, Gaussian post-filter smoothing with a full width at half maximum of 7 mm, 128 × 128 matrix, 3–5 min per bed position depending on BMI). Low-dose helical CT images were obtained for attenuation correction and anatomic localization.

All MRI examinations (SignaHDxt, Optima 450/450 W, or Discovery 750/750 W; GE Healthcare, Waukesha, WI, USA) were performed at either 1.5- or 3.0-Tesla with multiplanar T1-weighted (3–4 mm, TR/TE 700-900/minimum ms), fat-suppressed intermediate T2-weighted (3–4 mm, TR/TE 3000-6000/50), and post-gadolinium spoiled gradient (SPGR) (3–4 mm, TR/TE 100- 200/minimum ms) or fat-suppressed T1-weighted (3–4 mm, TR/TE 700-900/minimum ms) sequences with FOV and matrix size varying by lesion location.

MIM software (MIM Software Inc., Cleveland, OH, USA) was used for PET/CT analysis. ^{18}F-FDG PET/CT imaging characteristics included SUVmax, morphology of abnormal FDG activity (linear, nodular, fusiform), maximal dimensions of nerve abnormality, site of disease, and presence of other sites of disease. Examples of other sites of disease included lymph nodes, spleen, bone, or other peripheral nerves, and these sites were considered positive if metabolic activity exceeded that of the liver. MRI imaging characteristics included signal intensity on T1- and T2-weighted images (hypointense, isointense, hyperintense), enhancement pattern (solid, heterogeneous, non-enhancing), enhancement avidity (avid, moderate, mild, non-enhancing), morphology (linear, fusiform, nodular), and associated changes of muscle denervation (determined by the presence of increased T2-weighted signal, atrophy, and fatty replacement in muscles supplied by the involved nerve). Determination of signal intensity on T1 and T2-weighted images was compared to adjacent skeletal muscle.

The electronic medical record was searched and various other data were collected and analyzed, including patient age, gender, nerve biopsy results, bone marrow biopsy results, CSF analysis, history of prior treatment for lymphoma, and history of previous disease remission. The electronic medical record was also reviewed to assess for the presence of neoplasia other than lymphoma.

Statistical analysis was performed using JMP software on a Mac (JMP Pro, version 11.2.1, SAS Institute Inc.). Continuous variables are expressed as mean ± SD. Categorical variables are presented with absolute and relative frequencies. *P* values for between-group comparisons of continuous data were calculated from Kruskal–Wallis one-way analysis of variance (ANOVA). Statistical significance was established for *P* values of less than 0.05.

Results

Our search identified 27 cases from 25 unique patients with an average age of 64.6 ± 10.0 years (range, 47-87 years). Two patients had two separate sites of NL involvement that occurred greater than 1.5 years apart, with intervening disease remission. There were 18 males and seven females. ^{18}F-FDG PET/CT was performed in 26/27 cases (96%) and MRI was performed in 22/27 cases (81%). NL was proven by nerve biopsy in 23/27 cases (85%). Pathologic analysis of the biopsied nerve or histopathology from other sites (bone marrow, CSF, lymph node, solid organ, soft tissues) confirmed that all 27 cases were B-cell lymphoma; including 23/27 diffuse large B-cell lymphoma (85%), 2/27 mucosa-associated lymphoid tissue (MALT) lymphoma (7%), 1/27 low-grade B-cell lymphoma not otherwise specified (4%), and 1/27 mantle cell lymphoma (4%). No patient had a neoplasia other than lymphoma. Locations of NL involvement included 14/27 brachial plexus (52%) (Figs. 1 and 2), 7/27 sciatic nerve (26%) (Figs. 3 and 4), 5/27 lumbosacral plexus (19%), and 1/27 femoral nerve (4%) (Fig. 5). As part of staging, bone marrow biopsy was obtained in 19/27 cases (70%), and was negative in 17/19 cases (89%), whereas CSF analysis was obtained in 23/27 cases (85%), and was negative

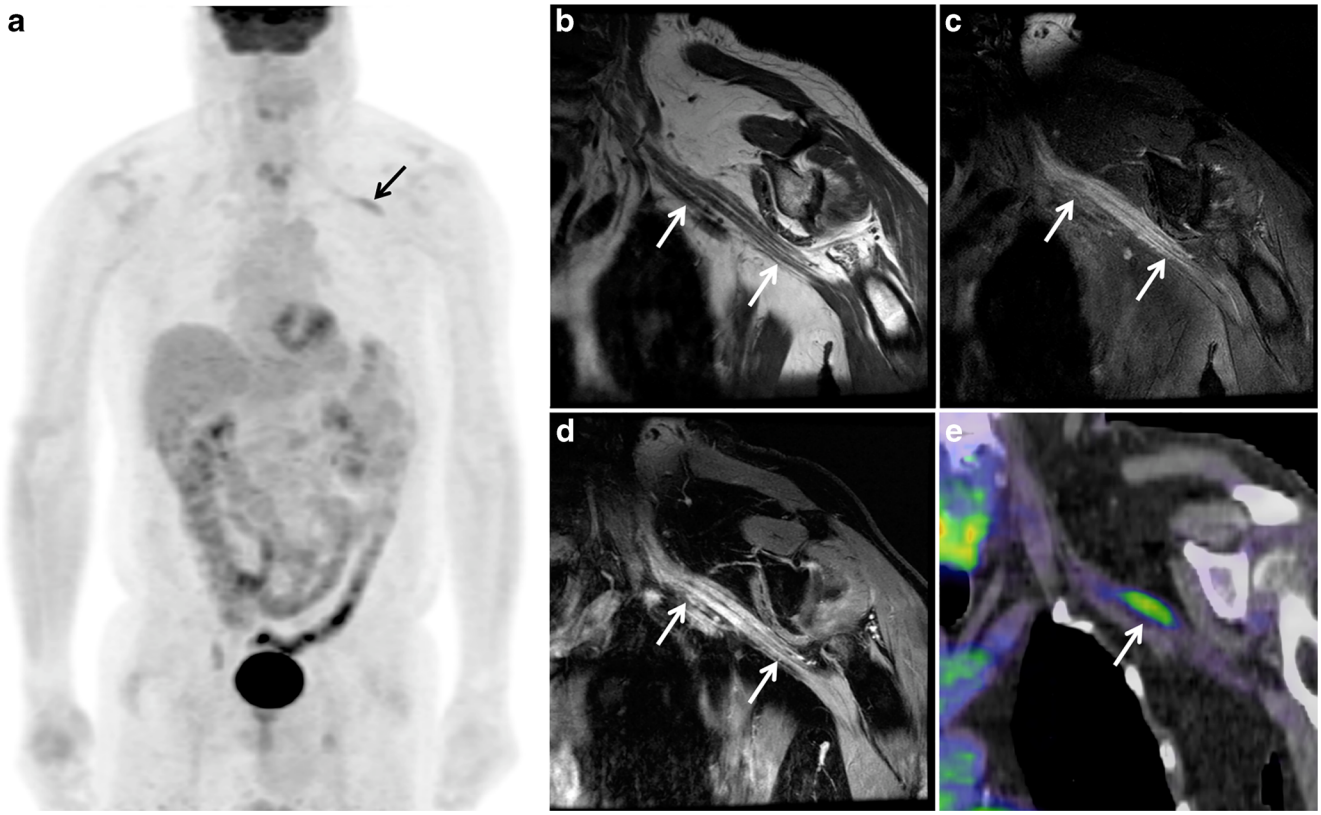

Fig. 1 A 60-year-old male with biopsy-proven B-cell NL of the left brachial plexus. FDG PET maximum intensity projection (MIP) (**a**), coronal MRI (**b**–**d**), and coronal fused PET/CT (**e**). Coronal oblique T1-weighted (**b**), T2-weighted fat-suppressed (FS) (**c**), and post-gadolinium FS spoiled gradient recalled (SPGR) (**d**) images demonstrate linear thickening of the left brachial plexus extending from the trunks through cords (*arrows*). Corresponding PET images (**a**, **e**) demonstrate a focal area of moderate FDG activity, SUVmax 3.5 (*arrows*), much more limited in extent than the MRI abnormality. The information provided by both modalities was used to guide fascicular biopsy, targeting the most FDG-avid region

in 16/23 (70%). A peripheral nerve was the sole site of disease in 18/27 cases (67%).

Treatment was administered at any point prior to imaging in 20/27 cases (74%); 7/27 cases (26%) had no prior history of lymphoma, and therefore represented cases of primary NL; in five of these seven cases, the peripheral nerves were the only site of involvement. Three of 27 cases (11%) had a documented history of prior peripheral nerve involvement that had resolved after therapy. Patients with a history of prior treatment were deemed to have been in remission at the time of PET/CT in 11/27 cases (41%). Five of 27 cases (19%) had received systemic chemotherapy less than 4 weeks prior to PET/CT.

^{18}F-FDG PET/CT morphology was characterized as linear in 14/26 cases (54%) (Figs. 1 and 5), fusiform in 6/26 (23%) (Figs. 2 and 3), nodular in 3/26 (12%) (Fig. 4), and mixed linear/nodular in 3/26 (12%). The average SUVmax was 7.1 ± 4.6 (range, 1.5–17.0). There was no significant difference in SUVmax between patients receiving prior chemotherapy (mean SUVmax 6.6 ± 4.8) and those without prior treatment (mean SUVmax 8.3 ± 4.0), $p = 0.43$; or in patients having received chemotherapy in the 4 weeks preceding PET/CT (mean SUVmax 4.2 ± 4.1) versus those without recent therapy (mean SUVmax 7.8 ± 4.5), $p = 0.12$. Involvement of other sites in addition to the peripheral nerves on PET/CT was present in 9/26 cases (35%); lymph nodes were positive in 3/26 (12%), spleen in 2/26 (8%), bone in 2/26 (8%), and various other locations in 8/26 (31%). These other locations included the soft tissues, submandibular gland, adrenal gland, lung, and central nervous system (brain and/or spinal cord). There was no significant difference in SUVmax between patients with disease at sites other than the peripheral nerves (mean SUVmax 8.3 ± 5.1) compared to those with isolated peripheral nerve involvement (mean SUVmax 6.4 ± 4.2), $p = 0.20$.

MRI morphology was characterized as linear in 11/22 cases (50%) (Figs. 1 and 5), fusiform in 6/22 (27%) (Figs. 2 and 3), nodular in 3/22 (14%) (Fig. 4), and mixed linear/fusiform in 2/22 (9%). The average maximum longitudinal dimension of the neural abnormality was 11.1 ± 5.9 cm (range, 3.5–23.0 cm), and the average maximum width dimension of the neural abnormality was 1.4 ± 0.73 cm (range, 0.5–3.4 cm). T1-weighted signal intensity relative to skeletal muscle was characterized as hypointense in 14/22 (64%), isointense in 7/22 (32%), and hyperintense in 1/22 (5%). T2-weighted signal intensity relative to skeletal muscle was characterized as

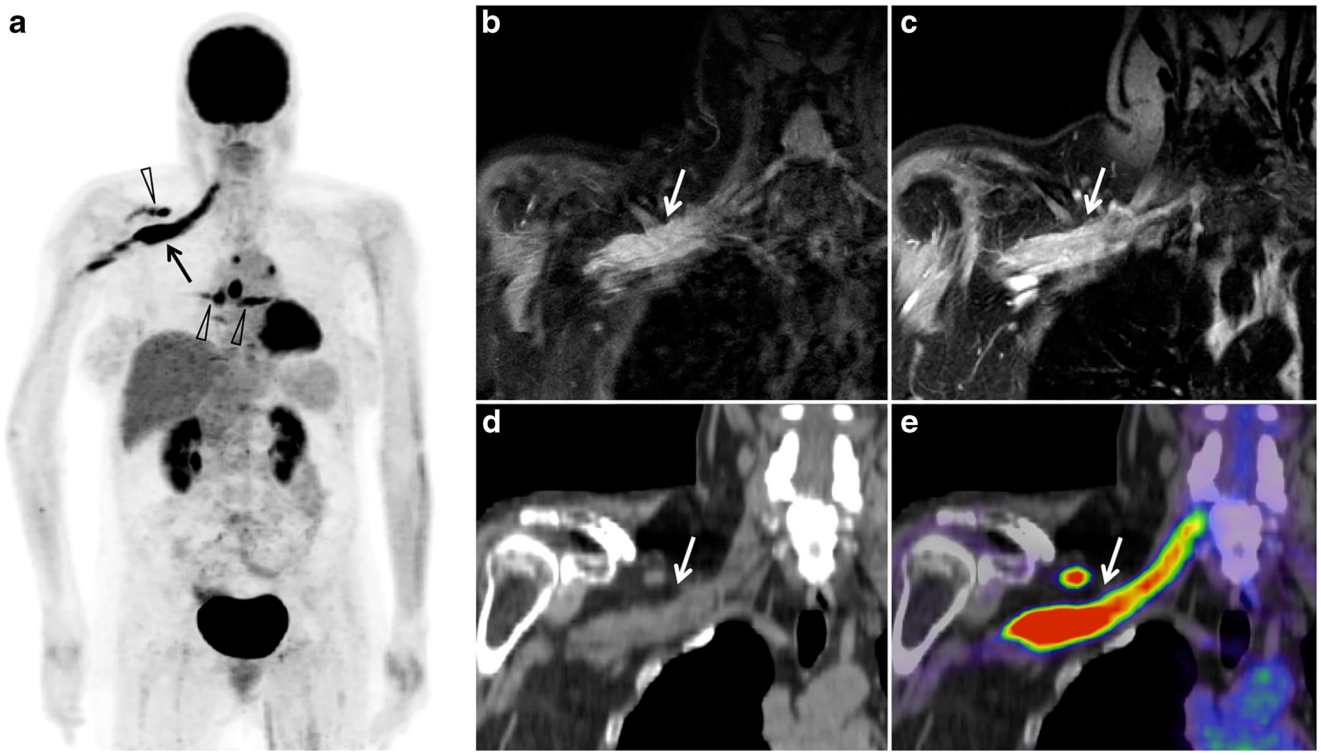

Fig. 2 A 51-year-old female with biopsy-proven diffuse large B-cell NL involving the right brachial plexus. FDG PET MIP (**a**), coronal MRI (**b**–**c**), coronal oblique CT (**d**), and coronal fused PET/CT (**e**). FDG PET images demonstrate fusiform thickening of the right brachial plexus, extending from the nerve roots through terminal branches (**a**, *arrow*) with intense FDG activity, SUVmax 12.7. There are several other areas of FDG avid peripheral nerve involvement (*arrowheads*, **a**). Coronal oblique T2-weighted FS (**b**) and post-contrast FS SPGR (**c**) images demonstrate thickening, T2-weighted hyperintensity and enhancement of the right brachial plexus (*arrows*). Coronal oblique CT (**d**) and fused FDG PET/CT images (**e**) demonstrate neural thickening and intense FDG activity (*arrows*)

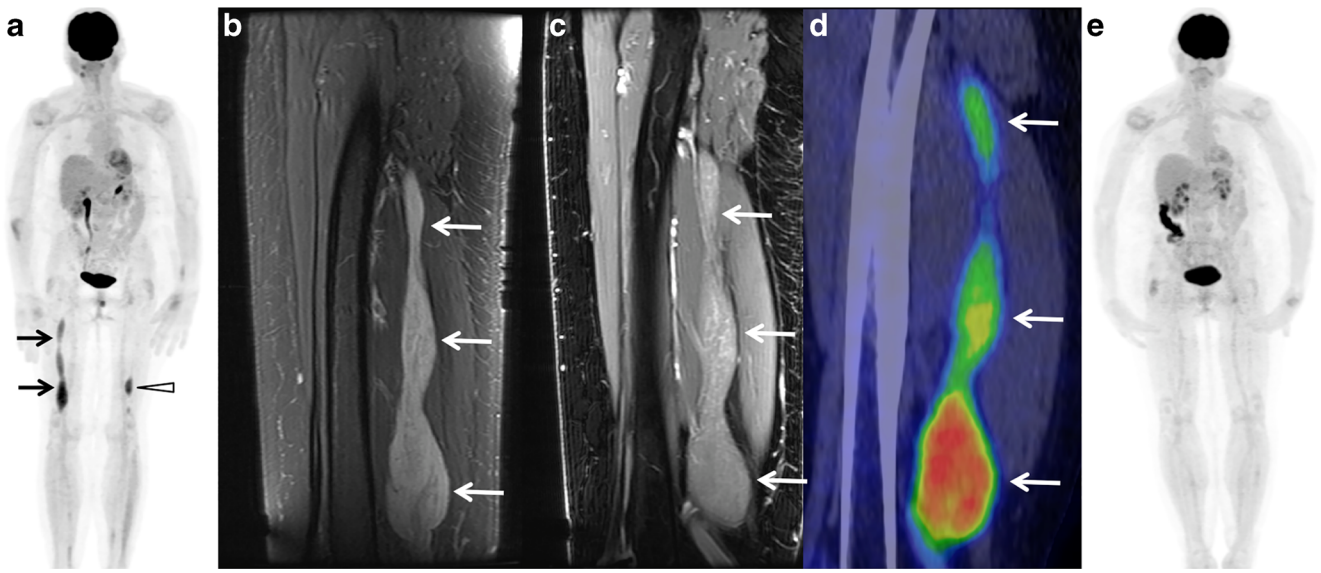

Fig. 3 A 68-year-old female with MALT lymphoma. FDG PET MIP (**a**), coronal MRI (**b**–**c**), coronal fused PET/CT (**d**), and subsequent FDG PET MIP following chemotherapy (**e**). Initial PET MIP (**a**) demonstrates fusiform increased FDG activity (SUVmax 5.1) along the course of the right sciatic nerve (*arrows*) and focal increased FDG activity in the left sciatic nerve (*arrowhead*). Sagittal T2-weighted FS (**b**) and post-contrast FS SPGR (**d**) images demonstrate fusiform enlargement, increased T2-weighted signal, and enhancement of the right sciatic nerve (*arrows*). PET MIP obtained 16 months after the initial scans and 14 months after completion of chemotherapy (**e**) demonstrates complete metabolic response

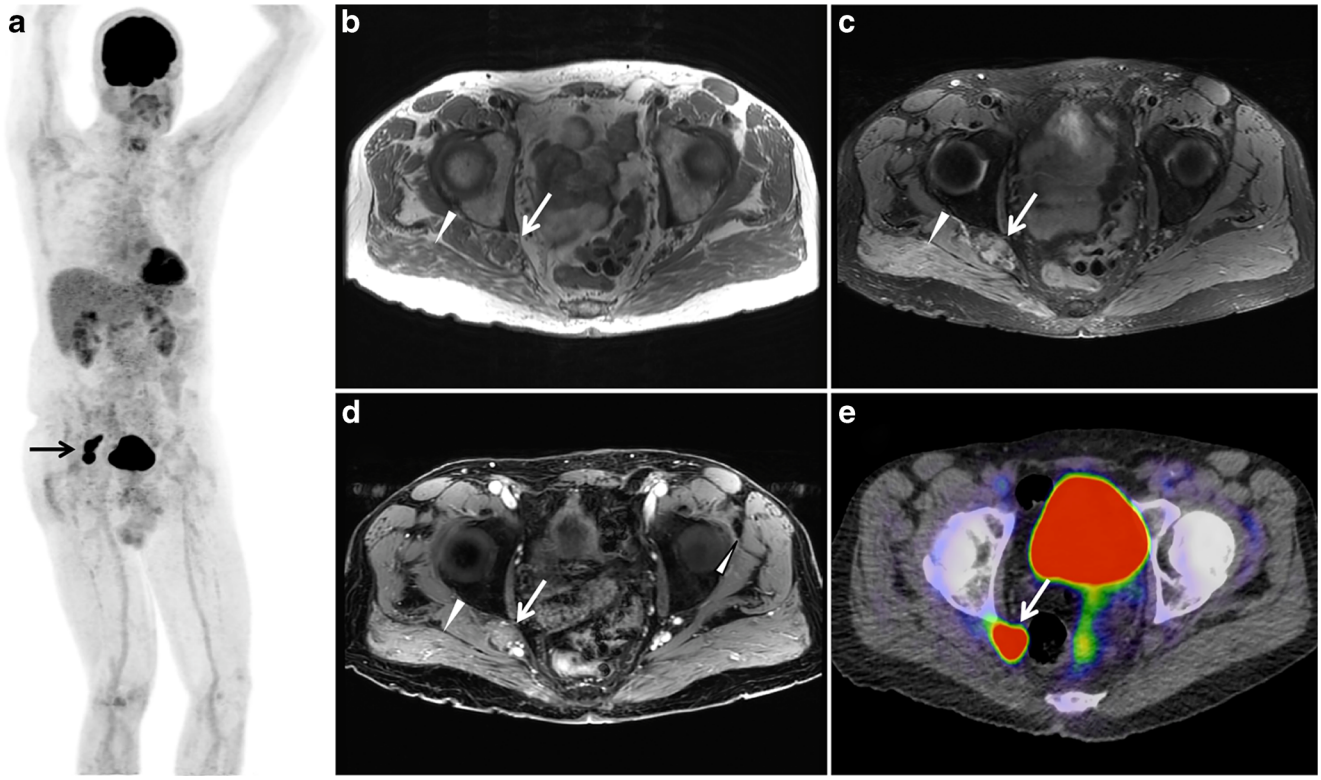

Fig. 4 A 74-year-old male with biopsy-proven diffuse large B-cell NL of the right sciatic nerve. FDG PET MIP (**a**), axial MRI (**b**–**d**), and axial fused PET/CT (**e**). PET images (**a**, **e**) demonstrate intense nodular FDG activity (SUVmax 15.8) involving the right sciatic nerve at the level of the sciatic notch (*arrows*), and no other areas of lymphoma. Axial T1-weighted (**b**), T2-weighted FS (**c**), and post-contrast FS SPGR (**d**) images demonstrate nodular enlargement of the proximal right sciatic nerve with increased T2-weighted signal and enhancement (*arrows*). Denervation changes are present in the right gluteus maximus muscle (*arrowheads*)

hyperintense in 21/22 (95%) and isointense in 1/22 (5%). The enhancement pattern was solid in 15/22 (68%), heterogeneous in 6/22 (27%), and non-enhancing in 1/22 (5%). The enhancement avidity was characterized as avid in 15/22 (68%), moderate in 4/22 (18%), and mild in 3/22 (14%). Associated changes of muscle denervation, including increased T2-weighted signal, atrophy, and fatty replacement were present in 14/22 cases (64%) (Figs. 4 and 5). There was no significant difference in the length of neural abnormality on MRI between those patients with muscular denervation and those without (mean SUVmax 10.4 ± 5.2 vs. 15.0 ± 6.4 cm, $p = 0.08$). FDG avidity in involved nerves was significantly higher in those patients with evidence of muscular denervation on MRI versus those without denervation changes (mean SUVmax 8.2 ± 4.6 vs. 4.3 ± 2.3, $p = 0.04$).

Discussion

NL affects the peripheral nerves, nerve roots, plexuses, or cranial nerves and typically manifests as a neuropathy. Most frequently NL occurs in the setting of known lymphoma, and less frequently as a primary manifestation of lymphoma [3, 8]. In a large single-center study, Davidson et al. found that 79% of their patients were diagnosed with NL after known lymphoma recurrence or progression, which is similar to 74% of patients in our study [15].

The diagnosis of NL can be challenging, as CSF and bone marrow analyses are frequently negative [10, 11]. In keeping with the literature, only 11% of patients with bone marrow biopsies and 30% of patients with CSF analysis were positive for lymphoma in this study. Given that other diagnostic tests are often negative, imaging has an important role in prompt and accurate diagnosis. One way imaging can expedite the diagnosis is by establishing a target for nerve biopsy. Using MRI to guide fascicular brachial plexus biopsies, Laumonerie et al. demonstrated an increased diagnostic yield [17]. Similarly, Capek et al. demonstrated a higher diagnostic yield of sciatic nerve biopsies using MRI to guide location [18]. In some cases, the extent of FDG activity was less extensive than the signal abnormality on MRI, potentially due to small volume disease and decreased spatial resolution of PET compared to MRI. Thus information from both exams could be used to better guide fascicular biopsy when compared to either modality alone (Fig. 1).

NL has a characteristic appearance on ^{18}F-FDG PET/CT. It generally presents as a linear or fusiform FDG-avid mass, following a neuronal path (Figs. 2, 3, and 5) [19, 20]. While

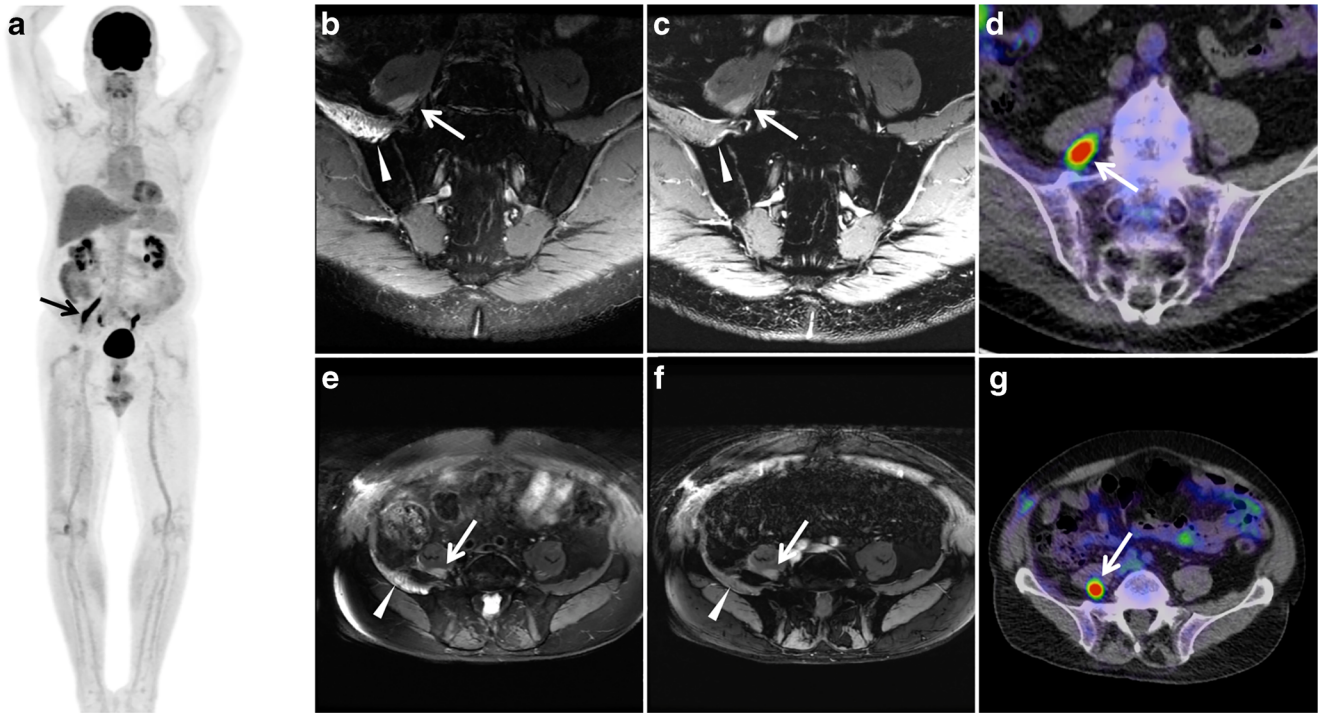

Fig. 5 A 66-year-old male with biopsy-proven diffuse large B-cell NL of the right femoral nerve. FDG PET MIP (**a**), coronal MRI (**b**–**c**), coronal fused PET/CT (**d**), axial MRI (**e**–**f**), and axial fused PET/CT (**g**). PET MIP image (**a**) shows an isolated site of intense linear FDG activity in the right pelvis (*arrow*). Oblique coronal and axial T2 FS (**b**, **e**), post-contrast FS SPGR (**c**, **f**), and fused PET/CT (**d**, **g**) images demonstrate linear enlargement, increased T2 signal, avid enhancement, and intense FDG activity (SUVmax 11.4) of the right femoral nerve (*arrows*). Note the associated denervation changes (*arrowheads*) of the right iliacus muscle

FDG activity can be variable (SUVmax range 1.5–17.0), NL is most often quite FDG-avid (average SUVmax 7.1). Davidson and colleagues found a nearly identical average level of metabolic activity (SUVmax 7.1, range, 2.3-10.8) as the patients in our cohort [15]. Salm et al. showed that NL has a tendency to affect the brachial and lumbar plexuses, peripheral nerves of the extremities, and the trigeminal nerve root [3]. Our findings were in agreement with the majority of cases affecting the brachial plexus (52%) (Figs. 1 and 2), and the remaining affecting the sciatic nerve (26%) (Figs. 3 and 4), lumbosacral plexus (19%), and femoral nerve (4%) (Fig. 5).

While NL is often diagnosed after disease progression or recurrence, in 67% of cases it was the only site of lymphoma at time of diagnosis. In patients without a history of treatment undergoing staging PET/CT, the peripheral nerves were the only site of involvement in 71% cases. Davidson et al. reported similar findings, with 63% of their patients presenting with single neural site involvement [15]. Prior studies have shown that nerves may act as a "safe lymphoma haven", as chemotherapeutic agents cannot cross the blood–nerve barrier [21]. Of our patients with a history of prior treatment, the peripheral nerves were the only site of relapse in 65%, and only 23% of these patients had a prior history of NL, supporting this concept. Therefore, when it occurs, NL is often the only site of lymphomatous involvement, independent of a history of prior treatment or of prior NL. Thus, even though NL is rare, those interpreting PET/CT should be aware of its presence, PET/CT appearance, and often-isolated nature.

The MRI findings of NL are even less well described in the literature. Several studies have shown that NL generally exhibits diffuse enlargement of the peripheral nerves or plexus, frequently with multifocal nodularity and T2-weighted hyperintensity [22–24]. Grisariu et al. found that the MRI findings of NL were nonspecific and included plexus or nerve enlargement with or without contrast enhancement [9]. Multiple other studies have described intense enhancement on post contrast T1-weighted images [23–26]. Capek et al. described a characteristic "tumefactive appearance" of NL as well as other hematologic malignancies including leukemia and plasmacytoma [27]. They defined a tumefactive appearance as complex, fusiform, T2-weighted hyperintense, circumferential tumor masses encasing the involved peripheral nerves. Our MRI findings were generally in keeping with the literature. Characteristic findings included T2-weighted hyperintensity (95%), enhancement (95%), and linear or fusiform thickening (86%) of the involved nerves. Associated changes of muscle denervation were present in the majority of cases (64%) (Fig. 4). Interestingly, we found significantly higher FDG activity on PET/CT in patients with evidence of muscular denervation on MRI than those without (mean SUVmax 8.2 vs. 4.3, $p = 0.04$), perhaps signaling more aggressive disease in patients with muscular denervation.

The diagnosis of NL is challenging, as there are many clinical differential diagnoses to consider. These include lymphoma-associated vasculitis, paraneoplastic neuropathy, peripheral nerve tumors, compressive neuropathy, radiation and chemotherapy induced neuropathy, and infection [2, 3, 8, 10, 14, 24]. The imaging characteristics of these various conditions can overlap, however the longitudinal extent, intense contrast enhancement on MRI, and degree of FDG-avidity of NL can lead to the correct diagnosis in the proper clinical context.

Limitations of the study include the small sample size and retrospective nature. Specifically, the limited number of patients in the subgroup analyses may be too small to reach statistical significance. Additionally, not all patients underwent both PET/CT and MRI. Patients with NL that did not resolve after chemotherapy were not included in the study, and their imaging findings might differ from those in this cohort. Another potential limitation is that more aggressive subtypes of B-cell NL may have been overrepresented. Future imaging studies including NL secondary to low-grade B-cell lymphomas and T-cell lymphomas would help to elucidate the full spectrum of this rare condition.

Conclusions

NL is a rare disease and a challenging diagnosis, as CSF and bone marrow analyses are frequently negative and numerous differential clinical diagnoses must be considered. The present study better defines the MRI and ^{18}F-FDG PET/CT imaging characteristics of NL, which most commonly manifests as T2-weighted hyperintense, enhancing linear or fusiform neural enlargement associated with muscular denervation on MRI, with intense FDG activity on PET/CT. It is most often an isolated site of disease, presenting after progression or recurrence. A familiarity with the imaging appearance of NL can help refine the differential diagnosis, direct biopsy, and aid in accurate diagnosis.

Compliance with ethical standards

Conflict of interest The authors declare that they have no conflicts of interest.

Ethical approval All procedures performed in studies involving human participants were in accordance with the ethical standards of the institutional and/or national research committee and with the 1964 Helsinki Declaration and its later amendments or comparable ethical standards.

Informed consent The need for informed consent was waived by the Institutional Review Board.

Publisher's Note Springer Nature remains neutral with regard to jurisdictional claims in published maps and institutional affiliations.

References

1. Baehring JM, Damek D, Martin EC, Betensky RA, Hochberg FH. Neurolymphomatosis. Neuro-Oncology. 2003;5(2):104–15.
2. Gan HK, Azad A, Cher L, Mitchell PL. Neurolymphomatosis: diagnosis, management, and outcomes in patients treated with rituximab. Neuro-Oncology. 2010;12(2):212–5.
3. Salm LP, Van der Hiel B, Stokkel MP. Increasing importance of 18F-FDG PET in the diagnosis of neurolymphomatosis. Nucl Med Commun. 2012;33(9):907–16.
4. Levin N, Soffer D, Grissaru S, Aizikovich N, Gomori JM, Siegal T. Primary T-cell CNS lymphoma presenting with leptomeningeal spread and neurolymphomatosis. J Neuro-Oncol. 2008;90(1):77–83.
5. Kosa SC, Peller PJ, Klein CJ. T-cell neurolymphomatosis involving cauda equina and sciatic nerves. Neurology. 2009;72(1):98.
6. Mahan MA, Ladak A, Johnston PB, Seningen JL, Amrami KK, Spinner RJ. Unique occurrence of mucosa-associated lymphoid tissue lymphoma disseminated to peripheral nerves. J Surg Orthop Adv. 2013;22(4):321–5.
7. Canh NX, Tan NV, Tung TT, Son NT, Maurea S. (18)F-FDG PET/CT in neurolymphomatosis: report of 3 cases. Asia Ocean J Nucl Med Biol. 2014;2(1):57–64.
8. Baehring JM, Batchelor TT. Diagnosis and management of neurolymphomatosis. Cancer J. 2012;18(5):463–8.
9. Grisariu S, Avni B, Batchelor TT, van den Bent MJ, Bokstein F, Schiff D, et al. Neurolymphomatosis: an International Primary CNS Lymphoma Collaborative Group report. Blood. 2010;115(24):5005–11.
10. Kanter P, Zeidman A, Streifler J, Marmelstein V, Even-Sapir E, Metser U, et al. PET-CT imaging of combined brachial and lumbosacral neurolymphomatosis. Eur J Haematol. 2005;74(1):66–9.
11. Lin M, Kilanowska J, Taper J, Chu J. Neurolymphomatosis—diagnosis and assessment of treatment response by FDG PET-CT. Hematol Oncol. 2008;26(1):43–5.
12. van den Bent MJ, de Bruin HG, Bos GM, Brutel de la Riviere G, Sillevis Smitt PA. Negative sural nerve biopsy in neurolymphomatosis. J Neurol. 1999;246(12):1159–63.
13. Hutchings M, Specht L. PET/CT in the management of haematological malignancies. Eur J Haematol. 2008;80(5):369–80.
14. Misdraji J, Ino Y, Louis DN, Rosenberg AE, Chiocca EA, Harris NL. Primary lymphoma of peripheral nerve: report of four cases. Am J Surg Pathol. 2000;24(9):1257–65.
15. Davidson T, Kedmi M, Avigdor A, Komisar O, Chikman B, Lidar M, et al. FDG PET-CT evaluation in neurolymphomatosis: imaging characteristics and clinical outcomes. Leuk Lymphoma. 2018;59(2):348–56.
16. Shree R, Goyal MK, Modi M, Gaspar BL, Radotra BD, Ahuja CK, et al. The diagnostic dilemma of neurolymphomatosis. J Clin Neurol. 2016;12(3):274–81.
17. Laumonerie P, Capek S, Amrami KK, Dyck PJ, Spinner RJ. Targeted fascicular biopsy of the brachial plexus: rationale and operative technique. Neurosurg Focus. 2017;42(3):E9.
18. Capek S, Amrami KK, Dyck PJ, Spinner RJ. Targeted fascicular biopsy of the sciatic nerve and its major branches: rationale and operative technique. Neurosurg Focus. 2015;39(3):E12.
19. Hong CM, Lee SW, Lee HJ, Song BI, Kim HW, Kang S, et al. Neurolymphomatosis on F-18 FDG PET/CT and MRI findings: a case report. Nucl Med Mol Imaging. 2011;45(1):76–8.
20. Trevisan AC, Ribeiro FB, Itikawa EN, Alexandre LS, Pitella FA, Santos AC, et al. 18F-FDG PET/CT/MRI fusion images showing cranial and peripheral nerve involvement in neurolymphomatosis. Indian J Nucl Med. 2017;32(1):77–8.
21. Dyck PJB, Suanprasert N, Mauermann M, Amrami K, Spinner R, Dyck P. Peripheral nerve lymphoma: clinical,

electrophysiological, radiographic and pathological findings. Neurology. 2015;84(24):P2.002.
22. Thawait SK, Chaudhry V, Thawait GK, Wang KC, Belzberg A, Carrino JA, et al. High-resolution MR neurography of diffuse peripheral nerve lesions. AJNR Am J Neuroradiol. 2011;32(8):1365–72.
23. Descamps MJ, Barrett L, Groves M, Yung L, Birch R, Murray NM, et al. Primary sciatic nerve lymphoma: a case report and review of the literature. J Neurol Neurosurg Psychiatry. 2006;77(9):1087–9.
24. Crush AB, Howe BM, Spinner RJ, Amrami KK, Hunt CH, Johnson GB, et al. Malignant involvement of the peripheral nervous system in patients with cancer: multimodality imaging and pathologic correlation. Radiographics. 2014;34(7):1987–2007.
25. Ahlawat S, Chhabra A, Blakely J. Magnetic resonance neurography of peripheral nerve tumors and tumorlike conditions. Neuroimaging Clin N Am. 2014;24(1):171–92.
26. Lim AT, Clucas D, Khoo C, Parameswaran BK, Lau E. Neurolymphomatosis: MRI and (18) FDG-PET features. J Med Imaging Radiat Oncol. 2016;60(1):92–5.
27. Capek S, Hebert-Blouin MN, Puffer RC, Martinoli C, Frick MA, Amrami KK, et al. Tumefactive appearance of peripheral nerve involvement in hematologic malignancies: a new imaging association. Skelet Radiol. 2015;44(7):1001–9.

One of the patients included in our cohort was previously included in a published article:

Capek S, Hebert-Blouin MN, Puffer RC, Martinoli C, Frick MA, Amrami KK, et al. Tumefactive appearance of peripheral nerve involvement in hematologic malignancies: a new imaging association. Skeletal Radiol. 2015; 44 [6]*:1001-1009.*

This publication was co-authored by one of the current manuscript's co-authors and the citation has been included in the manuscript.